Astronomical & Astrophysical Transactions

The Journal of the Eurasian Astronomical Society

Publication details, including instructions for authors and subscription information:
http://www.informaworld.com/smpp/title~content=t713453505

The galactic foreground angular spectra

A. V. Chepurnov

PLEASE SCROLL DOWN FOR ARTICLE

THE GALACTIC FOREGROUND ANGULAR SPECTRA

A. V. CHEPURNOV

Special Astrophysical Observatory Nizhnij Arkhyz, Karachai-Cherkess Republic, 357147, Russia

Galactic synchrotron and free–free foreground angular spectra are analytically estimated taking account of interstellar turbulence and radiating process physics. Unknown parameters of the spectra are obtained by fitting to observational data.

1 INTRODUCTION

The problem of Galactic screening foregrounds is of exclusive importance for CMB anisotropy experiments aiming to obtain basic cosmological parameters by an accurate measurement of Sakharov oscillations (Janke *et al.*, 1977; Jungman *et al.*, 1996a, b). The information about Galactic continuous emission is used to determine the radio frequency–angular scale region where CMB fluctuations dominate.

Present estimations of the most unclear aspect of this problem, angular spectra, are based on direct calculation from observational data and an empirical two-parameter (amplitude-angular spectrum index) spectrum model (Bersanelli *et al.*, 1996). However, applying this approach we encounter a lack of observational data and their low quality (for example, see Davies *et al.*, 1995), which can make direct angular spectrum estimations doubtful.

So it seems convenient to have a parametrization that accounts for radiating process physics. In this case we can incorporate essentially heterogeneous information, which can compensate primary data imperfections. In addition, as fitting parameters may have a physical meaning in this approach, we can find new information about interstellar media.

Working in this direction we did not find in existing publications a convenient analytical method allowing us to bind physical parameters of interstellar media with statistical properties of observed radio images, so a considerable part of this paper is devoted to the development of such a method.

2 SPECTRAL PROPERTIES OF THE GALACTIC RADIO EMISSION

2.1 Basic Terms

In this work we have to deal with different values and transforms involving stationary processes. The most convenient and in some cases the only way to obtain a desired result is to use a random process spectral representation (Ibragimov and Rozanov, 1970; Rozanov, 1963):

$$s(\mathbf{r}) = \int e^{i\mathbf{kr}} \Phi(d\mathbf{k}). \qquad (2.1.1)$$

where Φ is a stochastic spectral measure of a stationary process s.

This integral can be interpreted as a sum of flat waves, whose complex amplitudes are determined by a stochastic spectral measure of a wave vector space elementary volume, while these measure elements obey the following symbolic rule:

$$\Phi(d\mathbf{k})\Phi^*(d\mathbf{k}') = \delta_{\mathbf{k},\mathbf{k}'} F^2(\mathbf{k})\, d\mathbf{k}, \qquad (2.1.2)$$

where

$$\delta_{\mathbf{k},\mathbf{k}'} = \begin{cases} 0, & \mathbf{k} \neq \mathbf{k}' \\ 1, & \mathbf{k} = \mathbf{k}', \end{cases} \qquad (2.1.3)$$

and $F^2(\mathbf{k})$ is a power spectrum of a process s:

$$\overline{s(0)s(\mathbf{r})} = \int e^{i\mathbf{kr}} F^2(\mathbf{k})\, d\mathbf{k}. \qquad (2.1.4)$$

It is possible to employ an alternative *symbolic* form of the spectral representation, which is completely equivalent to the previous one:

$$s(\mathbf{r}) = \int e^{i\mathbf{kr}} F(\mathbf{k})\xi(\mathbf{k})\sqrt{d\mathbf{k}}, \qquad (2.1.5)$$

$$\overline{\xi(\mathbf{k})\xi^*(\mathbf{k}')} = \delta_{\mathbf{k},\mathbf{k}'}. \qquad (2.1.6)$$

We use the latter here despite the odious $\sqrt{d\mathbf{k}}$, as practice shows it to be more convenient.

We also assume the following to be correct for real random processes:

$$\xi(-\mathbf{k}) = \xi^*(\mathbf{k}), \qquad (2.1.7)$$

$$\overline{\xi^2(\mathbf{k})} = 0. \qquad (2.1.8)$$

2.2 Angular Spectrum through the Spatial Spectrum

We consider a model when an observer is located in the centre of some sphere filled with a luminous medium, and the radiation source function $s(\mathbf{r})$ is assumed to be a stationary random process with known power spectrum. The sphere is cut from

infinite space by some known function $w(r)$ of distance r from the sphere's centre, referred to as *the weighting function*. (This model is adequate if the respective variation of distance to the radiating medium edge is considerably less than unity at the considered angular scales.)

We are interested here in the angular spectrum of an observed image, given by the following function of angular coordinates:

$$S(\theta, \varphi) \equiv \int\limits_0^\infty w(r) s(r, \theta, \varphi)\, dr. \tag{2.2.1}$$

The source function will be replaced below by its spectral representation:

$$s(\mathbf{r}) = \int e^{i\mathbf{kr}} F(\mathbf{k}) \xi(\mathbf{k}) \sqrt{d\mathbf{k}}.$$

Let the original random process be isotropic. If so, accounting for

$$\mathbf{kr} = r \cdot (k_x \sin\theta \cos\varphi + k_y \sin\theta \sin\varphi + k_z \cos\theta)$$

we have the following expression for the angular autocorrelation function:

$$\begin{aligned}
C(\theta) &\equiv \overline{S(0,0) \cdot S^*(\theta, 0)} \\
&= \int\limits_0^\infty w(r)\, dr \cdot \int\limits_0^\infty w(r')\, dr' \cdot \int F(k) \sqrt{d\mathbf{k}} \\
&\times \int F(\mathbf{k}') \sqrt{d\mathbf{k}'} e^{i(-k_x' r' \sin\theta - k_y' r' \cos\theta + k_z' r)} \cdot \overline{\xi(\mathbf{k}) \xi^*(\mathbf{k}')}.
\end{aligned}$$

Having evaluated the averaging we derive:

$$C(\theta) = \int\limits_0^\infty w(r)\, dr \cdot \int\limits_0^\infty w(r')\, dr' \cdot \int F^2(k)\, d\mathbf{k} \cdot e^{i(-k_x' r' \sin\theta - k_y' r' \cos\theta + k_z' r)}.$$

After integration over the wave vector directions, we have the following expression:

$$C(\theta) = 4\pi \int\limits_0^\infty w(r)\, dr \cdot \int\limits_0^\infty w(r')\, dr' \int\limits_0^\infty k^2\, dk \cdot F^2(k) \cdot \frac{\sin k\sqrt{r^2 - 2rr'\cos\theta + r'^2}}{k\sqrt{r^2 - 2rr'\cos\theta + r'^2}}.$$

Taking account of

$$C_l^2 \equiv 2\pi \int\limits_0^\pi C(\theta) P_l(\cos\theta) \sin\theta\, d\theta. \tag{2.2.2}$$

we finally obtain the desired angular spectrum:

$$C_l^2 = 16\pi^2 \int\limits_0^\infty k^2\, dk \cdot F^2(k) \cdot \left(\int\limits_0^\infty j_n(kr) w(r)\, dr \right)^2. \tag{2.2.3}$$

We can see that the expression for the angular spectrum through the spatial spectrum takes the form of an integral transform with kernel being dependent of the weighting function.

However, this kernel is not convenient for direct computation because of an oscillating function (the spherical Bessel function $j_n(kr)$) in the integral. So it may be useful to find some direct analytical expression for it, with given adequate weighting function.

2.3 Kernel Approximation

Let $w(\mathbf{r})$ be Gaussian:

$$w(r) = e^{-\frac{r^2}{R^2}}, \tag{2.3.1}$$

where R is the distance from the luminous region edge. Then the transform may be written in the form:

$$C_l^2 = \frac{16\pi^2}{R} \cdot \int\limits_0^\infty u^2 \, du \cdot F^2(u/R) \cdot Q_l(u), \tag{2.3.2}$$

where

$$Q_l(u) \equiv \left(\int\limits_0^\infty j_l(u\nu) e^{-\nu^2} \, d\nu \right)^2. \tag{2.3.3}$$

Using the integral representation of the hypergeometric function,

$${}_1F_1(a;c;-1/z) = \frac{\Gamma(c)}{\Gamma(a)} \cdot z^a \int\limits_0^\infty e^{-zt} \cdot t^{a - \frac{(c+1)}{2}} \cdot J_{c-1}(2\sqrt{t}) \, dt,$$

we can find

$$Q_l(u) = \left[\frac{\sqrt{\pi}}{2u} \cdot \frac{\Gamma\frac{l+1}{2}}{\Gamma(\frac{2l+3}{2})} \cdot \left(\frac{u^2}{4} \right)^{\frac{l+1}{2}} \cdot {}_1F_1\left(\frac{l+1}{2}; \frac{2l+3}{2}; -\frac{u^2}{4} \right) \right]^2.$$

On the other hand, using the alternative integral form of ${}_1F_1$,

$${}_1F_1(a;c;z) = \frac{\Gamma(c)}{\Gamma(a)\Gamma(c-a)} \cdot \int\limits_0^1 e^{zt} \cdot t^{a-1} \cdot (1-t)^{c-a-1} \, dt,$$

we have:

$$Q_l(u) = \left(\frac{\sqrt{\pi}}{2u} \cdot \frac{\left(\frac{u^2}{4} \right)^{\frac{l+1}{2}}}{\Gamma\left(\frac{l+2}{2} \right)} \cdot \int\limits_0^1 e^{-\frac{u^2}{4}t} \cdot t^{\frac{l-1}{2}} \cdot (1-t)^{\frac{l}{2}} \, dt \right)^2.$$

Let us find an approximation for this expression for large l values. Let us denote

$$\mathcal{J} \equiv \left(\frac{u^2}{4}\right)^{\frac{l+1}{2}} \cdot \int_0^1 e^{-\frac{u^2}{4}t} \cdot t^{\frac{l-1}{2}} \cdot (1-t)^{\frac{1}{2}} \, dt \int_0^{u^2/4} e^{-z} \cdot z^{\frac{l-1}{2}} \cdot \left(1 - \frac{4z}{u^2}\right)^{\frac{l}{2}} \, dz.$$

Let $\alpha = \frac{u}{l}$ be constant:

$$\mathcal{J} = \int_0^{\alpha^2 l^2/4} e^{-z} \cdot z^{\frac{l-1}{2}} \cdot \left(1 - \frac{4z}{\alpha^2 l^2}\right)^{\frac{l}{2}} \, dz.$$

The integrand of the latter expression is positive and has a single maximum at $z_0 \approx l/2$ while $l \gg 1$, and with this condition the bulk of the area is located near the maximum. Since the maximum's form is affected only by the first two terms, the third one can be factored out of the integral with its value at z_0. Taking into account the fast decrease of the remaining integrand, we can spread the upper integration limit to infinity. So we have:

$$\mathcal{J} \approx \left(1 - \frac{2}{\alpha^2 l}\right)^{\frac{l}{2}} \cdot \int_0^\infty e^{-z} \cdot z^{\frac{l-1}{2}} \, dz = \left(1 - \frac{2}{\alpha^2 l}\right)^{\frac{l}{2}} \cdot \Gamma\left(\frac{l+1}{2}\right)$$

$$\approx \Gamma\left(\frac{l+1}{2}\right) \cdot e^{-\frac{1}{\alpha^2}},$$

$$Q_l(u) \approx \frac{\pi}{4u^2} \left(\frac{\Gamma\left(\frac{l+1}{2}\right)}{\Gamma\left(\frac{l+2}{2}\right)}\right)^2 \cdot e^{-2\frac{l^2}{u^2}}.$$

Using the gamma-function asymptotic,

$$\Gamma(z) \approx \sqrt{\frac{2\pi}{z}} \cdot e^{-z} \cdot z^z, \quad z \gg 1,$$

we finally obtain the following approximation of the kernel:

$$Q_l(u) \approx \frac{\pi}{2lu^2} \cdot e^{-2\frac{l^2}{u^2}}, \quad l \gg 1. \tag{2.3.4}$$

This approximation works with the appropriate precision for $l > 15$ uniformly over all 3-d wave vector values, so it can be used in the whole range where the original model is correct.

The following sections contain some special cases, important for practical applications.

2.4 Power Law 3-d Spectrum

If a source function has an unlimited power-law spectrum, the respective sphere projection also has a power-law spectrum, and the spectral indexes coincide:

$$F^2(k) = \frac{F_0^2}{k^\alpha}, \tag{2.4.1}$$

$$C_l^2 = \frac{4\pi^3 \Gamma\left(\frac{\alpha-1}{2}\right)}{2^{\frac{\alpha-1}{2}}} \cdot \frac{F_0^2 \cdot R^{\alpha-1}}{l^\alpha}. \tag{2.4.2}$$

Let us introduce some cut-off scale ("outer scale") L into the initial 3-d spectrum:

$$F^2(k) = \frac{F_0^2}{k^\alpha} \cdot e^{-\left(\frac{2\pi}{kL}\right)^2}. \tag{2.4.3}$$

In this case, the respective angular spectrum changes its spectral index from 1 for low l values to the spectral index of the source function for large ls in the vicinity of $l_0 = 2\pi R/L$:

$$C_l^2 = \frac{4\pi^3 \Gamma\left(\frac{\alpha-1}{2}\right)}{2^{\frac{\alpha-1}{2}}} \cdot \frac{F_0^2 \cdot R^{\alpha-1}}{l^\alpha \cdot \left(1 + \frac{1}{2}\left(\frac{2\pi R}{l \cdot L}\right)^2\right)^{\frac{\alpha-1}{2}}}. \tag{2.4.4}$$

A remarkable property of the spectrum (2.4.4) lies in the fact that opposite to the spectrum (2.4.2) an amplitude of a harmonic with fixed l is saturated when $R \to \infty$, which is caused by the influence of the outer scale L. Indeed, let us fix some angular scale β. Then at a distance more than L/β there will be no fluctuations exceeding the angle β, and the increase of distance R to the border of the radiating region over this limit will not cause an increase of the amplitude of an angular harmonic with typical scale β.

A decrease of the spectral index when going from small angular scales (large l values) to large ones (small l values) is explained by the same effect. Provided the distance L/β does not exceed R, the change (growth) of the angular harmonic with the increase of scale β occurs exclusively because of the increase of the amplitudes of spatial harmonics of the original random process at every distance inside the sphere of radius R (according to (2.4.3)). However, beginning with the angular scale $\beta_0 = L/R$, with further increase of β the "effective sphere" of radius L/β (i.e. the sphere, where the amplitude of the angular harmonic is formed) shrinks, which causes a slowing down of the increase of the respective angular harmonic amplitude.

The reason for the unit spectral index at low ls is directly seen from the expression (2.4.2): if with decreasing l (increasing β) we decrease the distance R proportionally to l, imitating the shrinking of the "effective sphere", then the spectrum will behave as l^{-1}.

2.5 The Case of a Squared Kolmogorov Process

Let the source function be a squared stationary random process with known properties:

$$s(\mathbf{r}) = \left(\overline{S} + \Delta S(\mathbf{r})\right)^2,$$

$$\Delta S(\mathbf{r}) = \int e^{i\mathbf{k}\mathbf{r}} \mathcal{F}(\mathbf{k})\xi(\mathbf{k})\sqrt{d\mathbf{k}}. \tag{2.5.1}$$

The respective autocorrelation function is equal to

$$
\begin{aligned}
C(\mathbf{r}) \;=\;& \overline{s(\mathbf{r})s(0)} \\[4pt]
=\;& \overline{\left(\overline{\mathcal{S}}^2 + 2\overline{\mathcal{S}}\cdot \int \sqrt{d\mathbf{k}_1'}\,e^{i\mathbf{kr}}\mathcal{F}(\mathbf{k}_1)\cdot\xi(\mathbf{k}_1)\right.} \\[4pt]
+\;& \overline{\int \sqrt{d\mathbf{k}_2}\,e^{i\mathbf{kr}}\mathcal{F}(\mathbf{k}_2)\cdot\xi(\mathbf{k}_2)\cdot\int\sqrt{d\mathbf{k}_3}\,e^{i\mathbf{kr}}\mathcal{F}(\mathbf{k}_3)\cdot\xi(\mathbf{k}_3)\left.\right)} \\[4pt]
\times\;& \overline{\left(\overline{\mathcal{S}}^2 + 2\overline{\mathcal{S}}\cdot \int \sqrt{d\mathbf{k}_1'}\,\mathcal{F}(\mathbf{k}_1')\cdot\xi(\mathbf{k}_1')\right.} \\[4pt]
+\;& \overline{\int \sqrt{d\mathbf{k}_2'}\,\mathcal{F}(\mathbf{k}_2')\cdot\xi(\mathbf{k}_2')\cdot\int\sqrt{d\mathbf{k}_3'}\,\mathcal{F}(\mathbf{k}_3')\cdot\xi(\mathbf{k}_3')\left.\right)}.
\end{aligned}
$$

According to (2.1.6), (2.1.7) and (2.1.8), let us write combinations of random variables ξ and respective wave vector combinations, giving a non-zero contribution:

(1) $\overline{\xi(\mathbf{k}_1)\xi(\mathbf{k}_1')}: \quad \mathbf{k}_1 = -\mathbf{k}_1';$

(2) $\overline{\xi(\mathbf{k}_2)\xi(\mathbf{k}_2')\xi(\mathbf{k}_3)\xi(\mathbf{k}_3')}:$

     (a) $\mathbf{k}_2 = -\mathbf{k}_2'$ and $\mathbf{k}_3 = -\mathbf{k}_3',$

     (b) $\mathbf{k}_2 = -\mathbf{k}_3'$ and $\mathbf{k}_3 = -\mathbf{k}_2',$

     (c) $\mathbf{k}_2 = -\mathbf{k}_3$ and $\mathbf{k}_2' = -\mathbf{k}_3';$

(3) $\overline{\xi(\mathbf{k}_2)\xi(\mathbf{k}_3)}: \quad \mathbf{k}_2 = -\mathbf{k}_3;$

(4) $\overline{\xi(\mathbf{k}_2')\xi(\mathbf{k}_3')}: \quad \mathbf{k}_2' = -\mathbf{k}_3'.$

The terms corresponding to the variants (2c), (3) and (4) are constant. As we are interested in a variable component only, these combinations (along with the other constant terms) will be omitted. Hence we derive (intersections of the variants correspond to sets of zero measure):

$$
C(\mathbf{r}) = (2\overline{\mathcal{S}})^2\cdot\int \mathcal{F}^2(\mathbf{k})e^{i\mathbf{kr}}\,d\mathbf{k} + 2\left(\int \mathcal{F}^2(\mathbf{k})e^{i\mathbf{kr}}\,d\mathbf{k}\right)^2. \tag{2.5.2}
$$

The respective power spectrum is equal to

$$
F^2(\mathbf{k}) \;=\; (2\overline{\mathcal{S}})^2\mathcal{F}^2(\mathbf{k}) + 2F_q^2(\mathbf{k}), \tag{2.5.3}
$$

$$
F_q^2(\mathbf{k}) \;\equiv\; \int \mathcal{F}^2(\mathbf{k}')\mathcal{F}^2(\mathbf{k}-\mathbf{k}')\,d\mathbf{k}'. \tag{2.5.4}
$$

So the source function power spectrum can be expressed through a sum of two terms, which may be referred to as *linear* and *quadratic*. The linear term is proportional to the power spectrum of the original random process, the quadratic one to the autoconvolution function of this spectrum.

Let us find an approximation for the quadratic term in the partial case when the original random process has a power-law spectrum with known outer scale and Kolmogorov spectral index:

$$\mathcal{F}^2(k) = \frac{\mathcal{F}_0^2}{k^{11/3}} \cdot e^{-\frac{k_0^2}{k^2}}. \tag{2.5.5}$$

Analysing the structure of expression (2.5.4) taking account of (2.5.5) we can assume that $F_q^2(\mathbf{k})$ must have the following asymptotics:

$$F_q^2(k) \approx \mathcal{F}_0^4 \mathcal{J}_0, \quad k \ll k_0,$$

$$F_q^2(k) \approx 2\mathcal{F}_0^4 \frac{\mathcal{J}_1}{k^{11/3}}, \quad k \gg k_0,$$

where

$$\mathcal{J}_0 \equiv \frac{4\pi}{\mathcal{F}_0^4} \int_0^\infty \mathcal{F}^4(k) k^2 \, d\mathbf{k},$$

$$\mathcal{J}_1 \equiv \frac{4\pi}{\mathcal{F}_0^2} \int_0^\infty \mathcal{F}^2(k) k^2 \, d\mathbf{k},$$

Now we can choose an approximation which fits the asymptotic conditions. A numerical evaluation shows that the following approximating function is adequate:

$$F_q^2(k) \approx \mathcal{F}_0^4 \frac{\mathcal{J}_0}{\left[\left(\frac{\mathcal{J}_0}{2\mathcal{J}_1}\right)^{6/11} k^2 + 1\right]^{11/6}}.$$

Having found the values of $\mathcal{J}_0$ and $\mathcal{J}_1$, we obtain:

$$F_q^2(k) \approx \frac{F_{q0}^2}{\left(a\frac{k^2}{k_0^2} + 1\right)^{11/6}}, \tag{2.5.6}$$

where

$$F_{q0}^2 \approx \frac{1.514\mathcal{F}_0^4}{k_0^{13/3}}, \quad a = 0.1842.$$

So for the angular spectrum of the quadratic term we have:

$$C_q^2(l) = \frac{8\pi^3}{Rl} \cdot \int_0^\infty e^{-2\frac{l^2}{u^2}} F_q^2\left(\frac{u}{R}\right) du = \frac{4\sqrt{2}\pi^3 F_{q0}^2}{2^{11/6} R \cdot \left(\frac{alL}{2\pi R}\right)^{11/3}} \int_0^\infty \frac{e^{-t} t^{1/3} \, dt}{\left[\frac{1}{2}\left(\frac{2\pi R}{alL}\right)^2 t + 1\right]^{11/6}}$$

($k_0 = \frac{2\pi}{L}$, L is outer scale).

We can find an approximation for the integral in the latter expression:

$$\int_0^\infty \frac{e^{-t}t^{1/3}\,dt}{\left(\frac{1}{2N^2}t+1\right)^{11/6}} \approx (3.21 \cdot e^{-3.34 \cdot N} + 1) \cdot \int_0^\infty e^{-t\cdot\left(1+\frac{11}{6}\frac{1}{2N^2}\right)}t^{1/3}\,dt$$

$$= (3.21 \cdot e^{-3.34 \cdot N} + 1) \cdot \frac{\Gamma\left(\frac{4}{3}\right)}{\left(1+\frac{11}{12N^2}\right)^{4/3}}.$$

So the angular spectrum of the quadratic term takes the following form:

$$C_q^2(l) = 1.48 \times 10^3 \cdot \frac{\mathcal{F}_0^4 \cdot R^{8/3}}{\left(\frac{2\pi}{L}\right)^{2/3}} \cdot \frac{1 + 3.21 \cdot e^{-1.43\frac{l \cdot L}{2\pi R}}}{l^{11/3} \cdot \left(1 + 5.0 \cdot \left(\frac{2\pi R}{l \cdot L}\right)^2\right)^{4/3}}. \tag{2.5.7}$$

This spectrum behaves analogously to the linear variant with the difference that its spectral index changes near the point $l_0 \approx 3 \cdot (2\pi R/L)$, instead of $l_0 = 2\pi R/L$ in the previous case, and its value is slightly bigger than unity in the region of lower ls. Saturation when $R \to \infty$ also takes place. These effects, as in the linear case, are explained by the divergence of the primary spectrum (2.5.6) from the pure power law.

Now we can write the full angular spectrum corresponding to the given source function:

$$C_I^2 = 1.76 \times 10^2 \cdot \frac{\overline{S}^2 \cdot \mathcal{F}_0^2 \cdot R^{8/3}}{l^{11/3} \cdot \left(1 + \frac{1}{2}\left(\frac{2\pi R}{l \cdot L}\right)^2\right)^{4/3}}$$

$$+ \ 2.96 \times 10^3 \cdot \frac{\mathcal{F}_0^4 \cdot R^{8/3}}{\left(\frac{2\pi}{L}\right)^{2/3}} \cdot \frac{1 + 3.21 \cdot e^{-1.43\frac{l \cdot L}{2\pi R}}}{l^{11/3} \cdot \left(1 + 5.0 \cdot \left(\frac{2\pi R}{l \cdot L}\right)^2\right)^{4/3}}. \tag{2.5.8}$$

3 GALACTIC SYNCHROTRON EMISSION

3.1 Source Function

The source function of galactic synchrotron emission is proportional to $B_\perp^{(\gamma+1)/2}$ (Eilek, 1989a, b; Weksler and Kellermann, 1976), where $B_\perp$ is the magnetic field projection on the image plane, and γ is the electron energy spectrum index. The latter is bound with the radio frequency intensity spectral index α by expression $\gamma = 2\alpha+1$. For the Galaxy $\alpha \approx 1$, and in this case the source function is proportional to the square of the perpendicular projection of the magnetic field.

On the other hand, from the theory of interstellar turbulence (Baum et al., 1958; Kaplan, 1958) it is known, that the Kolmogorov spectral index corresponds, in particular, to the quantity

$$\int d\Omega \sum_{l=1}^{3} G_{ll}(\mathbf{k}) \propto k^{-11/3},$$

where

$$G_{lm}(\mathbf{k}) \equiv \frac{1}{(2\pi)^3} \int B_{lm}(\mathbf{r}) e^{-i\mathbf{k}\mathbf{r}}\, d\mathbf{r}, \quad B_{lm}(\mathbf{r}) \equiv \overline{b_l(\mathbf{r}') b_m(\mathbf{r}' + \mathbf{r})}, \quad \mathbf{b} \equiv \frac{1}{\sqrt{4\pi\rho}} \cdot \mathbf{B},$$

ρ is the medium density. If we suggest $\rho \approx$ const, then

$$B_{lm}(\mathbf{r}) \approx \frac{1}{4\pi\rho} \overline{B_l(\mathbf{r}') B_m(\mathbf{r}' + \mathbf{r})}.$$

In the case of isotropic turbulence $B_{ll}(\mathbf{r})$ does not depend on the index l and the direction of $\mathbf{r}$ (Baum et al., 1958). In this case we have:

$$F_B^2(k) \propto k^{-11/3},$$

where $F_B^2(k)$ is the spatial power spectrum of the magnetic field component:

$$\overline{B_l(\mathbf{r}') B_l(\mathbf{r}' + \mathbf{r})} = \int F_B^2(k) e^{i\mathbf{k}\mathbf{r}}\, dk.$$

Hence, if our suggestions are correct, the magnetic field component has a Kolmogorov spectrum; and, then, if we assume that the orthogonal components of the image plane projection of the magnetic field are statistically independent, we can state that the synchrotron emission source function is proportional to the square of the Kolmogorov process (with zero mean).

3.2   Angular Spectrum

So, applying (2.5.7), we have the following expression for the synchrotron emission angular spectrum:

$$C_{\mathrm{syn}}^2(\lambda, l) = A \cdot \lambda^{5.8} \cdot \alpha^{8/3} \frac{1 + 3.21 \cdot e^{-1.43 \frac{l}{2\pi\alpha q}}}{l^{11/3} \cdot \left(1 + 5.0 \cdot \left(\frac{2\pi\alpha q}{l}\right)^2\right)^{4/3}} . \tag{3.2.1}$$

Here $\alpha \equiv R/R_P \approx 1/\sin|b|$, R_P is the distance to the radiating region border in the direction of the Galactic pole, $q \equiv R_P/L$, and λ is the wavelength in cm. The parameter α is introduced in order to account for the position of the observation site with respect to the Galactic plane.

If we have two observational data sets corresponding to non-coinciding angular frequency bands, we can estimate two unknown parameters of this spectrum, A and q. In this case, accounting to (A.8), we can write the following expression for the signal mean square for data sets with number $i = 1, 2$:

$$D_i = A \cdot \int \Phi_i^2(\kappa) F^2(\lambda_i, \alpha_i, q, \kappa)\, d\kappa, \tag{3.2.2}$$

where

$$F^2(\lambda, \alpha, q, \kappa) = \frac{\lambda^{5.8}\alpha^{8/3}}{(2\pi)^2} \cdot \frac{1 + 3.21 \cdot e^{-1.43\frac{\kappa}{2\pi\alpha q}}}{\kappa^{11/3} \cdot \left(1 + 5.0 \cdot \left(\frac{2\pi\alpha q}{\kappa}\right)^2\right)^{4/3}},$$

and $\Phi_i(\kappa)$ is an agular filter.

Let us rewrite (3.2.2) in the following form:

$$A = D_i \cdot f_i(q), \tag{3.2.3}$$

where

$$f_i(q) \equiv \left(\int \Phi_i^2(\kappa) F^2(\lambda_i, \alpha_i, q, \kappa)\, d\kappa\right)^{-1}.$$

So every data set yields the respective dependence $A(q)$, and their intersection point gives an estimation of values of A and q.

We used here two one-dimensional data sets corresponding to wavelengths 7.6 cm (Parijskij and Korolkov, 1986, see Figure 1) and 21 cm (Davies *et al.*, 1995, see Figure 2).
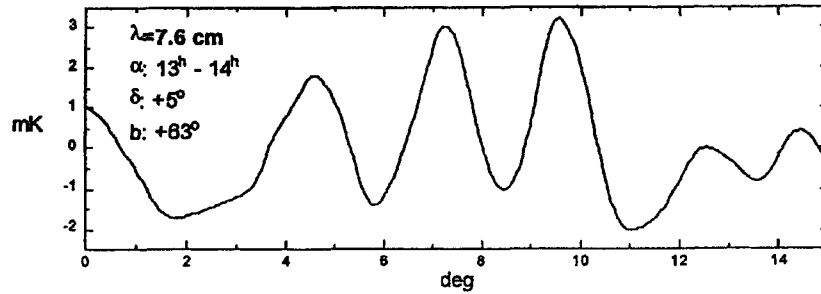
Figure 1   The Cold-80 experimental data (RATAN-600 radio telescope). The angular scale range 1–5° is determined by data processing (Parijskij and Korolkov, 1986).
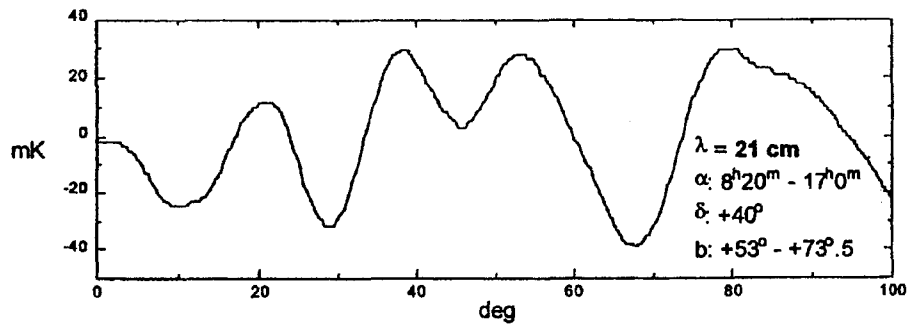
Figure 2   The 1420 GHz survey data convoluted with a triple beam (beam separation ±8°, HPBW = 5°). Discrete sources were previously removed (Davies *et al.*, 1995).

For the RATAN-600 data we accounted for the aperture efficiency $\varepsilon_a = 0.78$ and for all non-synchrotron components (discrete sources, free–free emission, dust emission) obtained by computer simulation (Chepurnov, 1995; Parijskij and Chepurnov, 1995) overall r.m.s. is estimated as 0.47 mK. Finally we obtained:

$$\lambda_1 = 7.6 \text{ cm}, \quad D_1 = 1.72 \times 10^{-6} \text{ K}^2, \quad \alpha_1 = 1.12,$$

$$\Phi_1(\kappa) = \left(1 - e^{-\frac{\kappa_x^2}{4a_1^2}}\right) e^{-\frac{\kappa_x^2}{4a_0^2}}$$

where $a_0 = \frac{2\sqrt{\ln 2}}{0.017}$, $a_1 = \frac{2\sqrt{\ln 2}}{0.087}$. For the second data set the respective parameters are:

$$\lambda_2 = 21 \text{ cm}, \quad D_2 = 3.88 \times 10^{-4} \text{ K}^2, \quad \alpha_2 = 1.13,$$

$$\Phi_2(\kappa) = (1 - \cos \kappa_x d)e^{-\frac{\kappa^2}{4a^2}},$$

where $a = \frac{2\sqrt{\ln 2}}{0.087}$, $d = 0.140$.

Now an intersection point can be found (see Figure 3) and this gives

$$A = 1.04 \times 10^{-6}, \quad q = 14.0. \tag{3.2.4}$$
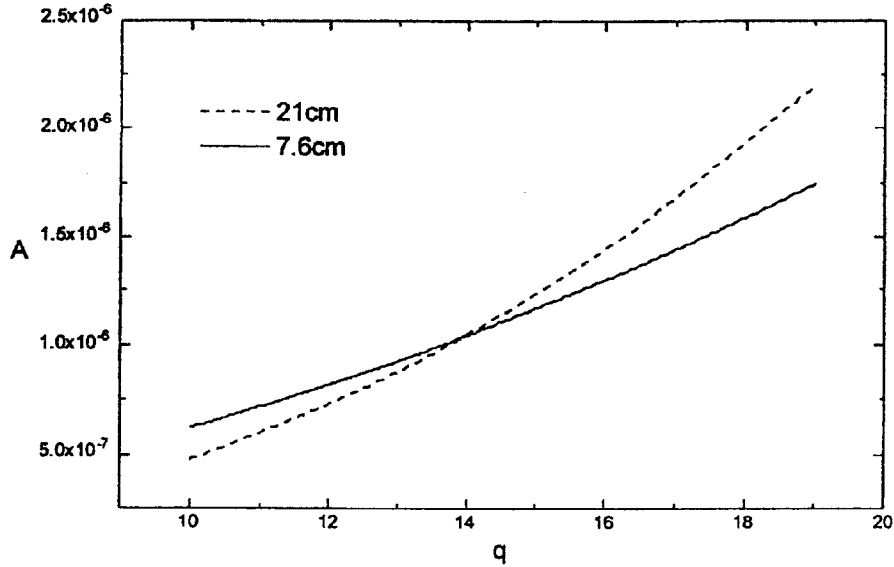
Figure 3 $A(q)$ functions corresponding to the considered data sets.

3.3   A Confidence Interval for R/L

It is clearly seen from Figure 4 that small deviations of D_i can cause a significant change of A and q. So it is highly advisable to find a confidence interval of estimated q and an accuracy of the corresponding spectrum (3.2.1).
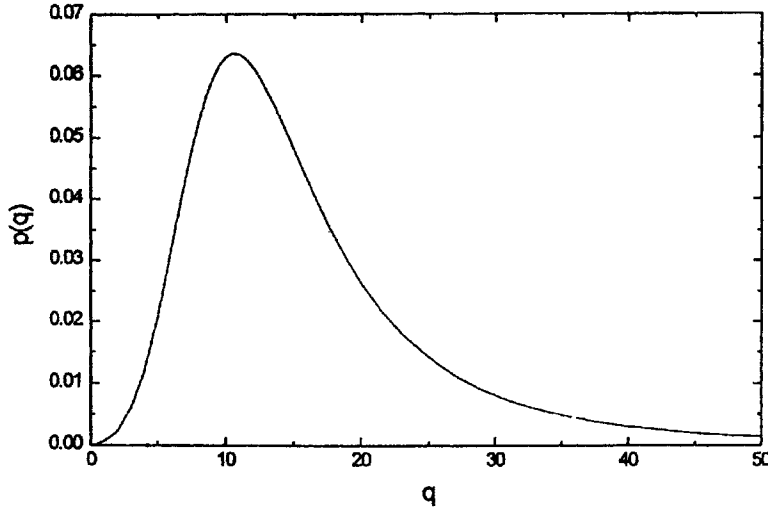
Figure 4 Probability density of the parameter $q = R/L$.

Using (B.3), we can estimate standard deviations of D_i:

$$\sigma_{D_1} = 5.3 \times 10^{-7} \text{ K}^2, \quad \sigma_{D_2} = 1.1 \times 10^{-4} \text{ K}^2.$$

To simplify calculations we assume that D_i values have normal distribution. In this case the mutual probability distribution for D_i has the following form (D_i are statistically independent because the data sets correspond to different sky regions):

$$P_D(D_1, D_2) = \frac{1}{2\pi\sigma_{D_1}\sigma_{D_2}} e^{-\frac{(D_1 - \overline{D}_1)^2}{2\sigma_{D_1}^2}} e^{-\frac{(D_2 - \overline{D}_2)^2}{2\sigma_{D_2}^2}} .$$

The respective elementary probability is

$$dP = p_D(D_1, D_2)\, dD_1\, dD_2.$$

For the area of an image of the square $dD_1 dD_2$ on the plane $\{(q, A)\}$, projected by transform (3.2.3), we can write the following:

$$ds = \frac{f_1(q) f_2(q)}{|D_1 f_1'(q) - D_2 f_2'(q)|}\, dD_1\, dD_2.$$

Accounting for (3.2.3), we can find the mutual probability density of A and q:

$$p(q, A) = \frac{dP}{dS} = A \cdot \frac{\left|\frac{f_1'(q)}{f_1(q)} - \frac{f_2'(q)}{f_2(q)}\right|}{f_1(q) f_2(q)} \cdot p_D\left(\frac{A}{f_1(q)}, \frac{A}{f_2(q)}\right). \tag{3.3.1}$$

Integrating this numerically over A, we obtain the probability density distribution of q (see Figure 4).

So we can now estimate a confidence interval. Finally we have:

$$R/L = 14.0^{+11.8}_{-5.7} \qquad (3.3.2)$$

for the confidence probability 0.68.

This error is not caused by measurement accuracy and can be reduced only by enlarging the observational areas.

The corresponding spectrum error is $\pm16\%$ for $l = 100$, $\pm39\%$ for $l = 320$ and $\pm48\%$ for $l = 1000$.

3.4 The Result

The angular spectrum, calculated according to (3.2.1) and (3.2.4), is shown in Figure 5 along with the empirical spectrum from the COBRAS/SAMBA project (Bersanelli et al., 1996), obtained from 408 MHz and 1420 MHz survey data.
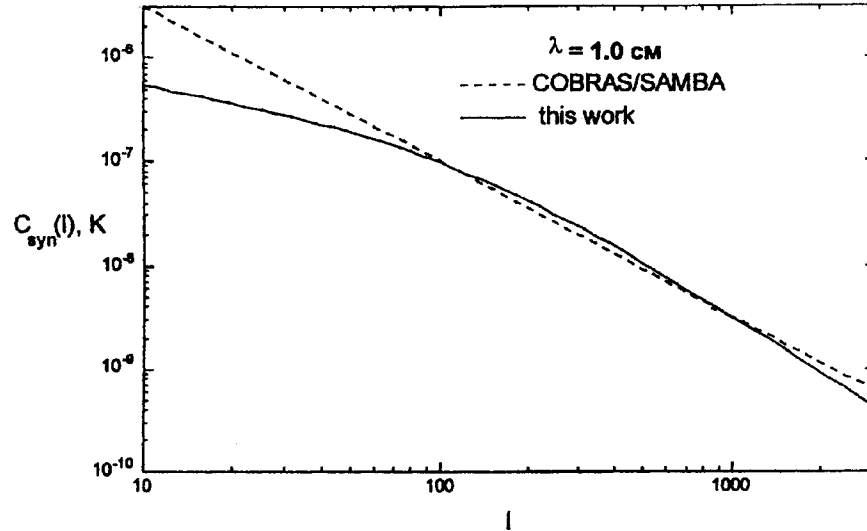
Figure 5 Angular spectrum of Galactic synchrotron emission.

We can suggest that the spectral index 3 found by Bersanelli et al., (1996) is caused by the influence of the outer scale L and corresponds to a transition from a spectral index of about unity at low ls to a Kolmogorov index of $11/3$ when $l \to \infty$.

4 GALACTIC FREE-FREE EMISSION

4.1 Source Function

In the case of free-free emission the source function is proportional to the squared electron density (Kaplan and Pikelner, 1979). The respective brightness tempera-

ture is expressed through the line-of-sight integral from the electron density in the following way:

$$T_{ff} = 4.8 \times 10^{-6} \cdot \lambda^{2.16} \cdot \int_{l.o.s} n_e^2 \, dr, \qquad (4.1.1)$$

where λ is measured in cm, n_e in cm^{-3}, r in pc, T_{ff} in K.

On the other hand, it is known from pulsar emission scintillation measurements that electron density fluctuations have a Kolmogorov power spectrum:

$$F_e^2(k) = \frac{F_0^2}{k^{-11/3}}$$

where $k \geq 2\pi/L$ and L is an outer scale.

The amplitude of the spectrum is estimated by Cordes et $al.$ (1991)

$$F_0^2 = 3.16 \times 10^{-4} m^{-20/3},$$

if k is measured in m^{-1}.

So for the Galactic free–free emission angular spectrum we can use the result from Section 2.5.

4.2 Angular Spectrum

Applying (2.5.8) to (4.1.1) we have the following expression for the free-free emission angular spectrum:

$$C_{ff}^2(\lambda, l) = 4.0 \times 10^{-10} \cdot \lambda^{4.32} \cdot \frac{\overline{n_e}^2 \cdot F_0^2 \cdot R^{8/3}}{l^{11/3} \cdot \left(1 + 0.5 \cdot \left(\frac{2\pi R}{l \cdot L}\right)^2\right)^{4/3}}$$

$$+ \, 6.65 \times 10^{-10} \cdot \lambda^{4.32} \cdot \frac{F_0^4 \cdot R^{8/3}}{\left(\frac{2\pi}{L}\right)^{2/3}} \cdot \frac{1 + 3.21 \cdot e^{-1.43\frac{l \cdot L}{2\pi R}}}{l^{11/3} \cdot \left(1 + 5.0 \cdot \left(\frac{2\pi R}{l \cdot L}\right)^2\right)^{4/3}} \qquad (4.2.1)$$

where $\overline{n_e} = 0.05$ cm^{-3} is the mean electron density, $F_0^2 = 3.16 \times 10^{-4} m^{-20/3}$ is the electron density spatial power spectrum amplitude, and R and L are measured in pc, λ in cm, and the result in K^2. For R one can assume $R = 1000/\sin|b|$ pc, where b is the Galactic latitude (Cordes et $al.$, 1991).

The only remaining unknown parameter is L, the outer scale of turbulence. To estimate it we can use the signal r.m.s. value over some observation site. Using (A.7) we have the following expression for this value over a circular region with radius a:

$$\sigma^2 = \frac{1}{2\pi} \int_0^\infty \left(1 - \left[\left(\frac{2}{ak}\right) J_1(ak)\right]^2\right) C_{ff}^2(\lambda, k) k \, dk. \qquad (4.2.2)$$

If σ^2 is known, one can fit the parameter L of the spectrum (4.2.1) to satisfy (4.2.2). The observational site shape does not affect it much (for non-pathological
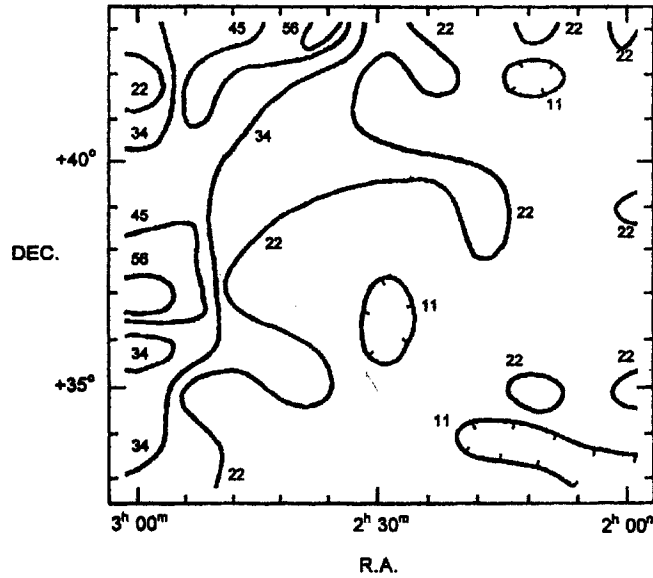
Figure 6 Brightness temperature of Galactic free–free emission in μK at $\lambda = 1$ cm obtained by recounting from the H_α intensity (Reynolds, 1992).

shapes); for other shapes one can choose a in order to make the areas equal. To determine the outer scale L we used H_α data, recounted to the free–free emission (see Figure 6, Reynolds, 1992). For $\sigma = 11.2$ μK, $b = -21°$, $a = 6°2$ fitting with (4.2.2) gives

$$L = 214\,\text{pc}. \qquad (4.2.3)$$

The free–free emission angular spectrum given by (4.2.1) taking account of (4.2.3) is displayed in Figure 7 along with the spectrum obtained by Bersanelli *et al.* (1996). We can see that this spectrum is 5–10 times lower than the CO-BRAS/SAMBA estimation. The slope corresponding to a spectral index of 3 from Bersanelli *et al.* (1996) is observed only in the region $30 < l < 200$; for larger l it corresponds to the Kolmogorov spectral index.

5 SUMMARY

So the main results of the present work are as follows:

(1) A transform converting the 3-d spatial spectrum of the source function to the angular spectrum of the observed image found in its general form (2.2.3). Also a convenient approximate expression for this transform is found for a Gaussian weighting function (2.3.2, 2.3.4).
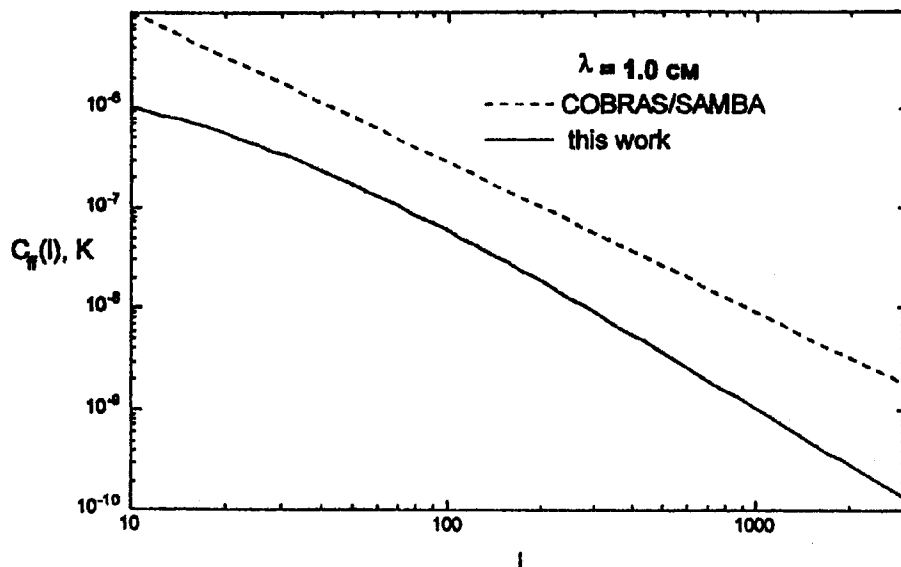
Figure 7 The Galactic free–free emission angular spectrum.

(2) Angular spectra of the synchrotron and free–free Galactic radio emission are obtained with general assumptions about their source functions (3.2.1, 4.2.1).

(3) Free parameters of these spectra are found by fitting to observational data. Information about the turbulence outer scale is found for a random magnetic field (3.3.2) and electron density (4.2.3).

However, we must note the following disadvantages of the obtained results:

(1) As the behaviour of the interstellar medium parameters, spatial spectra at scales bigger than the turbulence outer scale is still not estimated, a cut-off such as the one used in (2.4.3) does not seem to be well-founded. So the outer scales found here may be regarded only as order-of-magnitude estimations.

(2) Fitting of the synchrotron angular spectrum involves only a small part of the existing observational data, and may be regarded as a demonstration of the method rather than as final result.

(3) The final estimations show that H_α fluctuations are mostly caused by the geo-corona structure, and if this is true, then the free–free emission angular spectrum found here may be considered only as an upper limit, along with the corresponding outer scale.

So we can now state that free–free emission has an angular spectrum lying at least one order of magnitude lower than the present estimation of the CO-BRAS/SAMBA project, which shifts to lower radio frequencies the optimal band of

CMB anisotropy experiments, and makes it possible to measure the CMB angular spectrum even at short centimetre wavelengths.

References

Baum, F. A., Kaplan, S. A., and Staniukowich, K. P. (1958) *Introduction to Space Gas Dynamics*, Fizmatgiz, Moscow (in Russian).
Bersanelli, M. *et al.* (1996) *COBRAS/SAMBA, A Mission Dedicated to Imaging the Anisotropies of Anisotropies of the Microwave Background*, Preprint ESA D/SCI(96)3.
Chepurnov, A. V. (1995) Preprint SAO RAS No. 107SPb (in Russian).
Cordes, J. M. *et al.* (1991) *Nature* **354**, 121.
Davies, R. D., Watson, R. A., and Gutierres, C. M. (1995) Jodrell Bank Preprint No. 1215.
Eilek, J. A. (1989a) *Astron. J.* **98**, 244.
Eilek, J. A. (1989b) *Astron. J.* **98**, 256.
Ibragimov, I. A. and Rozanov, Yu. A. (1970) *Gaussian Random Processes*, Nauka, Moscow (in Russian).
Janke, E., Emde, F., and Loesch, F. (1977) *Special Functions*, Nauka, Moscow (in Russian).
Jungman, G. *et al.* (1996a) *Harvard–Smithsonian Center for Astrophysics*, Preprint No. 4237.
Jungman, G. *et al.* (1996b) *Phys. Rev. Lett.* **76**, 1007.
Kaplan, S. A. (1958) *Interstellar Gas Dynamics*, Fizmatgiz, Moscow (in Russian).
Kaplan, S. A. and Pikelner, S. B. (1979) *Physics of Interstellar Medium*, Nauka, Moscow (in Russian).
Parijskij, Yu. N. and Chepurnov, A. V. (1995) *Space Sci. Rev.* **74**, 269.
Parijskij, Yu. N. and Korolkov, D. V. (1986) In: R. A. Syunyaev (ed.) *Itogi Nauki i Tekhniki, Ser. "Astronomija"* **31**, 73 (in Russian).
Reynolds, R. J. (1991) *Astrophys. J.* **372**, L17.
Reynolds, R. J. (1992) *Astrophys. J.* **392**, L35.
Rozanov, Yu. A. (1963) Stationary Random Processes, Fizmatgiz, Moscow (in Russian).
Weksler, G. L. and Kellermann, K. I. (eds.) (1976) *Galactic and Extragalactic Radioastronomy*, Mir, Moscow (in Russian).

Appendix A.   Estimation of the Dispersion over a Selected Region

Let $s(\mathbf{r})$ to be a real random process with spectral representation

$$s(\mathbf{r}) = \int e^{i\mathbf{kr}} F(\mathbf{k})\xi(\mathbf{k})\sqrt{dk}.$$

Let Ω to be a limited region in space $\{\mathbf{r}\}$. Then

$$
\begin{aligned}
D_\Omega &\equiv \left\langle (s - \langle s\rangle_\Omega)^2 \right\rangle_\Omega = \frac{1}{\mu} \int_\Omega \left(s(\mathbf{r}) - \frac{1}{\Omega}\int_\Omega s(\mathbf{r}')d\mathbf{r}' \right)^2 d\mathbf{r} \\
&= \int F(\mathbf{k})\xi(\mathbf{k})\sqrt{dk} \cdot \int F(\mathbf{k}')\xi(\mathbf{k}')\sqrt{dk'} \cdot \left(\Pi_\Omega(\mathbf{k}+\mathbf{k}') - \Pi_\Omega(\mathbf{k})\Pi_\Omega(\mathbf{k}') \right)
\end{aligned} \tag{A.1}
$$

where

$$\Pi_\Omega(\mathbf{k}) \equiv \frac{1}{\Omega} \int_\Omega e^{i\mathbf{kr}} \, d\mathbf{r}. \tag{A.2}$$

We assume below that the region Ω is symmetrical with respect to coordinate inversion (in this case $\Pi_\Omega(\mathbf{k})$ is a real function) and contains 0.

Taking account of this assumption we can write some other properties of $\Pi_\Omega(\mathbf{k})$:

$$\Pi_\Omega(0) = 1, \tag{A.3}$$

$$\Pi_\Omega(-\mathbf{k}) = \Pi_\Omega(\mathbf{k}), \tag{A.4}$$

$$\int \Pi_\Omega(\mathbf{k}) \, d\mathbf{k} = \frac{(2\pi)^n}{\Omega}, \tag{A.5}$$

$$\int \Pi_\Omega^2(\mathbf{k}) \, d\mathbf{k} = \frac{(2\pi)^n}{\Omega}. \tag{A.6}$$

where n is the dimension of $\{\mathbf{r}\}$.

For rough estimations it is convenient to assume that $\Pi_\Omega(\mathbf{k})$ is equal to unity in some vicinity of 0 of volume $\frac{(2\pi)^n}{\Omega}$, and is equal to zero at all other points.

Having averaged $(A.1)$ taking account of $(2.1.6)$, $(2.1.7)$, $(2.1.8)$, $(A.3)$ and $(A.4)$ we have:

$$\overline{D_\Omega} = \int F^2(\mathbf{k}) \left(1 - \Pi_\Omega^2(\mathbf{k}) \right) d\mathbf{k}. \tag{A.7}$$

If we can neglect harmonics with a characteristic scale larger than the dimension of Ω, the second multiplicand in the latter expression can be omitted:

$$\overline{D_\Omega} \approx \int F^2(\mathbf{k}) \, d\mathbf{k}. \tag{A.8}$$

Appendix B.   Standard Deviation of the Estimated Dispersion

Taking account of $(A.1)$, we can write the following:

$$
\begin{aligned}
\sigma_D^2 &\equiv \overline{\left(D_\Omega - \overline{D_\Omega}\right)^2} = \overline{D_\Omega^2} - \overline{D_\Omega}^2 \\
&= \int F(\mathbf{k})\sqrt{dk} \cdot \int F(\mathbf{k}')\sqrt{dk'} \cdot \int F(\mathbf{k}_1)\sqrt{dk_1} \cdot \int F(\mathbf{k}_1')\sqrt{dk_1'} \\
&\quad \times \left(\Pi_\Omega(\mathbf{k}+\mathbf{k}') - \Pi_\Omega(\mathbf{k})\Pi_\Omega(\mathbf{k}') \right) \left(\Pi_\Omega(\mathbf{k}_1+\mathbf{k}_1') - \Pi_\Omega(\mathbf{k}_1)\Pi_\Omega(\mathbf{k}_1') \right) \cdot \\
&\quad \times \overline{\xi(\mathbf{k})\xi(\mathbf{k}')\xi(\mathbf{k}_1)\xi(\mathbf{k}_1')} - \overline{D_\Omega^2}.
\end{aligned}
$$

Then, with $(2.1.6)$, $(2.1.7)$ and $(2.1.8)$, we can write wave vector combinations giving a non-zero contribution to $\overline{D_\Omega^2}$:

(1) $\mathbf{k} = -\mathbf{k}'$ and $\mathbf{k}_1 = -\mathbf{k}'_1$,

(2) $\mathbf{k} = -\mathbf{k}_1$ and $\mathbf{k}' = -\mathbf{k}'_1$,

(3) $\mathbf{k} = -\mathbf{k}'_1$ and $\mathbf{k}' = -\mathbf{k}_1$.

Variant (1) yields $\overline{D^2_\Omega}$ (see $(A.7)$) and cancels; combinations (2) and (3) give an equal result. So we have:

$$\sigma^2_D = 2 \int F^2(\mathbf{k}) d\mathbf{k} \cdot \int F^2(\mathbf{k}')\, d\mathbf{k}' \cdot \left(\Pi_\Omega(\mathbf{k} + \mathbf{k}') - \Pi_\Omega(\mathbf{k}) \Pi_\Omega(\mathbf{k}') \right)^2, \qquad (B.1)$$

and, again, if harmonics with a characteristic scale larger than the dimension of Ω are negligible, the latter expression can be simplified. As $F(\mathbf{k})$ is even, we have:

$$\sigma^2_D \approx 2 \int F^2(\mathbf{k}) d\mathbf{k} \cdot \int F^2(\mathbf{k}')\, d\mathbf{k}' \cdot \Pi^2_\Omega(\mathbf{k} - \mathbf{k}'). \qquad (B.2)$$

If we suppose that the region where $\Pi^2_\Omega(\mathbf{k} - \mathbf{k}')$ with fixed $\mathbf{k}'$ significantly non-zero is small enough to neglect spectrum variations within it, then with $(A.6)$ we have the following approximate expression:

$$\sigma^2_D \approx 2 \frac{(2\pi)^n}{\Omega} \int F^4(\mathbf{k})\, d\mathbf{k}. \qquad (B.3)$$